

PROCEEDINGS OF SPIE

[SPIDigitalLibrary.org/conference-proceedings-of-spie](https://spiedigitallibrary.org/conference-proceedings-of-spie)

Lateral inhibition in magnetic domain wall racetrack arrays for neuromorphic computing

Cui, Can, Akinola, Otitoaleke , Hassan, Naimul, Bennett, Christopher, Marinella, Matthew, et al.

Can Cui, Otitoaleke G. Akinola, Naimul Hassan, Christopher H. Bennett, Matthew J. Marinella, Joseph S. Friedman, Jean Anne C. Incorvia, "Lateral inhibition in magnetic domain wall racetrack arrays for neuromorphic computing," Proc. SPIE 11470, Spintronics XIII, 1147011 (20 August 2020); doi: 10.1117/12.2568870

SPIE.

Event: SPIE Nanoscience + Engineering, 2020, Online Only

Lateral inhibition in magnetic domain wall racetrack arrays for neuromorphic computing

Can Cui^a, Otitoaleke G. Akinola^a, Naimul Hassan^b, Christopher H. Bennett^c, Matthew J. Marinella^c, Joseph S. Friedman^b, and Jean Anne C. Incorvia^a

^aThe University of Texas at Austin, Austin, TX, United States

^bThe University of Texas at Dallas, Richardson, TX, United States

^cSandia National Laboratory, Albuquerque, NM, United States

ABSTRACT

Neuromorphic computing captures the quintessential neural behaviors of the brain and is a promising candidate for the beyond-von Neumann computer architectures, featuring low power consumption and high parallelism. The neuronal lateral inhibition feature, closely associated with the biological receptive field, is crucial to neuronal competition in the nervous system as well as its neuromorphic hardware counterpart. The domain wall - magnetic tunnel junction (DW-MTJ) neuron is an emerging spintronic artificial neuron device exhibiting intrinsic lateral inhibition. This work discusses lateral inhibition mechanism of the DW-MTJ neuron and shows by micromagnetic simulation that lateral inhibition is efficiently enhanced by the Dzyaloshinskii-Moriya interaction (DMI).

Keywords: magnetism, spintronics, lateral inhibition, winner-take-all, domain wall racetrack, spin transfer torque, neuromorphic computing,

1. INTRODUCTION

The von Neumann architecture, as today's mainstream computer architecture, features serial execution mode and physically separated computation and memory locations known as the "memory wall"¹. Although the computation power of the von Neumann machine has increased tremendously over the past decades, the von Neumann memory wall still limits the computational speed and results in high energy consumption, which calls for a shift in computation paradigm. Biology-inspired neuromorphic computing is promising for addressing the discrepancy between the computation power of the human brain and computers in certain cognitive tasks. In neuromorphic computing, the memory wall dissolves as the neuron is both the computation and data storage unit; also, multiple neurons are connected through numerous synapses that store the weights of connections and can be modified according to synaptic learning rules. The high parallelism and the compute-in-memory nature make the neuromorphic system highly suitable for data-intensive artificial intelligence applications²³.

Signal processing of the nervous system requires the selective firings of a group of neurons in order to distinguish between different stimuli. The firing group selection is based on the winner(s)-take-all (WTA) rule(s) that limit the number of firing neuron(s) (winner) in the population. *Hard*-WTA selects only one neuron with the largest total input stimuli as the winner. In the biologically plausible local neural circuitry model⁴, this type of WTA is most frequently employed. Two other types of WTA, namely *k*-WTA, in which $k > 1$ winners are chosen, and *soft*-WTA, in which the neuron outputs are analog, have been shown to outperform the classical threshold perceptron⁵. It has also been proposed that the $E\%$ -max WTA is a more robust description of the group selection mechanism⁶.

WTA is implemented via neuron inhibition (i.e. the winning neurons exert inhibitory forces on other competitors and prevent their firing). Specifically, *lateral* inhibition is the mutual inhibition of the neurons belonging to the same layer, and is crucial to the auditory cortex, somatosensory cortex and vision.⁷ In many biologically plausible models, lateral inhibition is mediated by an interneuron, which performs a surround-type inhibition

Further author information: (Send correspondence to Jean Anne C. Incorvia)

Jean Anne C. Incorvia: E-mail: incorvia@austin.utexas.edu, Telephone: 1 737 808 4124

upon other neurons once it receives the output from the winner⁴⁸. The WTA-via-lateral inhibition feature has been realized in the CMOS VLSI platform^{9,10} and more recently in a hybrid CMOS-memristor crossbar array.¹¹ However, these implementations require peripheral circuitry and recurrent connections between the neurons, which greatly increase the area and power overhead of the chip, especially for large-scale networks.

A new form of neuron interaction is the key to an efficient and low-power lateral inhibition implementation. Spintronics based on emerging magnetic materials offers a new arena of novel neuromorphic device development. The domain wall - magnetic tunnel junction (DW-MTJ) neuron is an artificial leaky integrate-and-fire spiking neuron based on the three-terminal MTJ (3T-MTJ) device.¹² It consists of a DW racetrack that performs neuronal integration and an MTJ that outputs the spiking signals. The low power consumption of the DW motion device has been demonstrated in both device- and circuit-level simulations^{13,14}; moreover, the leaking and lateral inhibition functionalities are implemented without extra energy cost: leaking is implemented with a shared fixed ferromagnetic layer¹⁵ or racetrack shape gradient,¹⁶ lateral inhibition originates from magnetostatic interaction^{15,17} and is intrinsic to the DW-MTJ neuron. We also showed previously¹⁷ that the magnitude of lateral inhibition is maximized by optimizing the magnetostatic interaction strength and the material parameters of a DW-MTJ neuron pair. Here, we first review the mechanisms of DW-MTJ lateral inhibition; we then show that the Dzyaloshinskii-Moriya interaction (DMI) is highly efficient in further enhancing the lateral inhibition.

2. RESULTS

2.1 Maximized lateral inhibition in a pair of DW-MTJ neurons

In the DW-MTJ neuron, the DW position of the DW racetrack encodes the neuron activity and determines the magnetic stray field of the device; thus in a pair of side-by-side DW-MTJ neurons (Fig. 1(a) cartoon), the magnetic environment experienced by a DW is determined by its position relative to its neighbor. In Fig. 1(a), the two DWs (Neurons) are referred to as DW_I (Neuron I), the DW (Neuron) of Interest, and DW_N (Neuron N), the Neighbor DW (Neuron), respectively. The two DWs propagate along $+x$ driven by spin-transfer torque (STT). The less active DW_I lags behind DW_N and is thus subjected to a stray field along $-z$ originating from the $+z$ domain of Neuron N; reciprocally, DW_N experiences a stray field along $+z$ originating from the $-z$ domain of Neuron I.

To show the stray field dependence on the DW positions, we calculate the z - component of the stray field B_z ¹⁸ experienced by DW_I (see Table.1 for parameters). In Fig. 1(b)-(e), DW_N is located at $X_N = 1 \mu\text{m}$, $2 \mu\text{m}$, $3 \mu\text{m}$ and $4 \mu\text{m}$ respectively; for each X_N , B_z is plotted against the DW_I position X_I . It is seen that B_z is of negative sign when $X_I < X_N$ and of positive sign when $X_I > X_N$, indicating that the inactive DW experiences a stray field along $-z$ while the active DW experiences a stray field along $+z$. We have shown¹⁷ that only the $-z$ stray field plays a role in lateral inhibition. It is also worth noting that except around the DW racetrack ends and the narrow DW regions, B_z is highly uniform along x . This allows us to conveniently model the influence of Neuron N as a uniform external magnetic field B_{ext} , its direction dependent on the relative activities of the two neurons.

Lateral inhibition of the DW-MTJ neuron is manifested in DW velocity reduction (Δv_{DW}). The Landau-Lifshitz-Gilbert (LLG) equation dictates that DW velocity is determined by the combined effects of the electrical charge current density and magnetic field. The STT-driven DW velocity (v_{DW}) can thus be controlled by an external magnetic field (B_{ext}): in the v_{DW} vs. B_{ext} characteristics¹⁷, a below- Walker breakdown (WB) regime¹⁹ is observed. This regime is bounded by the low WB field (B_{WL}) and the high WB field (B_{WH}), and is characterized by a high DW mobility $\mu = dv_{\text{DW}}/d|B_{\text{ext}}|$. It is in this regime that v_{DW} exhibits the largest magnetic field tunability: v_{DW} decreases with increasing $-z$ external field until it reaches the B_{WL} . Therefore, the maximum lateral inhibition is achieved with a neighbor neuron stray field of B_{WL} , which is realized by choosing the optimal neuron spacing s_0 . s_0 varies with device material and geometry parameters; for the DW-MTJ neuron with fixed parameters, the maximized Δv_{DW} is:¹⁷

$$\Delta v_{\text{DW}} = -2\pi\gamma\delta M_S K_{\perp}$$

where γ is the gyromagnetic ratio, δ the DW width, M_S the saturation magnetization and K_{\perp} the in-plane magnetic anisotropy.

Table 1. Parameters used in micromagnetic simulations

DW racetrack dimensions ($x \times y \times z$)	$5 \mu\text{m} \times 50 \text{nm} \times 1.3 \text{nm}$
simulation cell size	$2 \text{nm} \times 5 \text{nm} \times 1.3 \text{nm}$
DW racetrack spacing s (Fig. 1(b)-(e))	90 nm
exchange stiffness A_{ex}	$13 \times 10^{-12} \text{J m}^{-1}$
saturation magnetization M_z	1.6 T
perpendicular magnetic anisotropy (PMA) K_U	10^6J m^{-3}
charge current density J_e (Fig. 2)	$2.2 \times 10^{12} \text{A m}^{-2}$
Gilbert damping α	0.02
non-adiabaticity β	0.04
spin polarization P	0.72
interfacial Dzyaloshinskii-Moriya interaction (DMI) (Fig. 2)	-0.5mJ m^{-2}

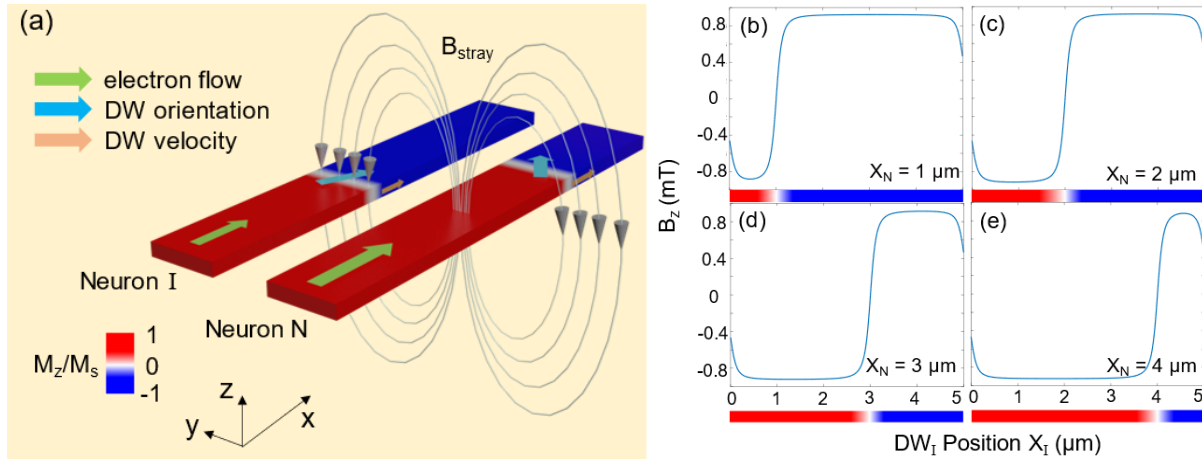


Figure 1. Magnetostatic interactions of a pair of DW-MTJ neurons. (a) Schematics of two side-by-side DW-MTJ neurons, with the coordinate system used throughout the article and magnetic moment defined by legend. Only the DW racetracks are shown. Here Neuron N is more active and impedes the motion of DW_I. (b)-(e) Stray field component B_z experienced by DW_I versus DW_I position X_I , for DW_N located at positions $X_N = 1 \mu\text{m}$, $2 \mu\text{m}$, $3 \mu\text{m}$ and $4 \mu\text{m}$.

2.2 Enhanced lateral inhibition with Dzyaloshinskii-Moriya interaction (DMI)

As discussed in 2.1, the maximum lateral inhibition is limited by the WB of the DW. It is therefore possible to further enhance lateral inhibition of the DW-MTJ neuron by suppressing WB. The Dzyaloshinskii-Moriya interaction (DMI) has been experimentally observed to stabilize a chiral Néel-type DW²⁰ and suppress its WB. Fig. 2 shows the influence of interfacial DMI on the v_{DW} versus B_{ext} characteristics. Here the DW motion of an isolated neuron is simulated using the Mumax³ micromagnetic simulation package²¹ (see Table. 1 for simulation parameters), and the influence of the neighboring neuron is modeled by applying a vertical external field B_{ext} . From here two roles of the DMI can be summarized. First, it increases the WB fields: in the absence of DMI (blue squares), the WB fields are $B_{\text{WL}} = -0.9 \text{mT}$ and $B_{\text{WH}} = -0.1 \text{mT}$; while with DMI (red circles), the WB fields increase to $B_{\text{WL}} = -1.4 \text{mT}$ and $B_{\text{WH}} = 0.4 \text{mT}$. Second, the DMI enhances the field tunability of v_{DW} : in the absence of DMI (blue squares), v_{DW} has the range $[v_{\text{min}}, v_{\text{max}}] = [20 \text{ms}^{-1}, 120 \text{ms}^{-1}]$; with DMI, the velocity range is increased to $[-43 \text{ms}^{-1}, 184 \text{ms}^{-1}]$. Notably, a negative-sign DW velocity is achieved with DMI, indicating that the lateral inhibition is strong enough not only to delay the neuron firing time but also reverse the direction of DW motion and strictly prohibit the neuron from firing.

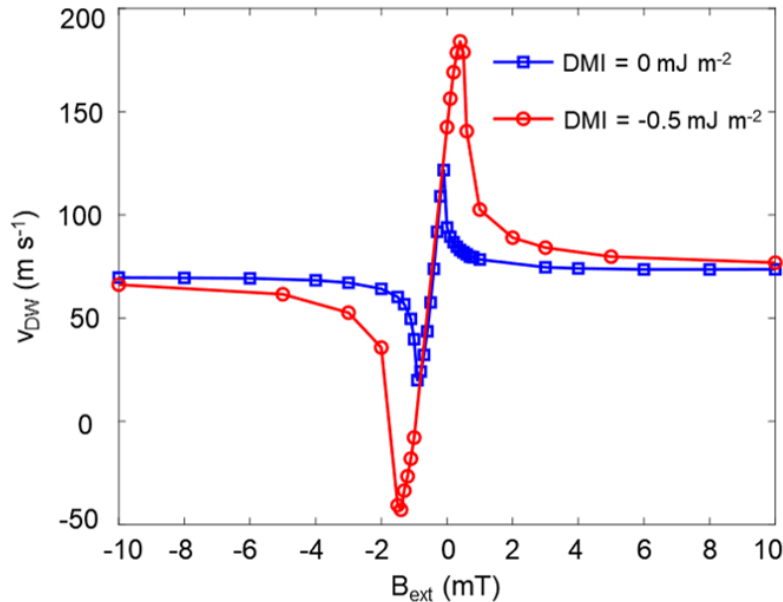


Figure 2. The current-driven DW velocity (v_{DW}) versus external magnetic field (B_{ext}) characteristics of an isolated DW racetrack, with interfacial Dzyaloshinskii-Moriya interaction (DMI) = 0 (blue squares) and DMI = -0.5 mJ m^{-2} (red circles).

3. CONCLUSIONS

This work studies the lateral inhibition characteristics of the domain wall - magnetic tunnel junction (DW-MTJ) neuron. Lateral inhibition of the DW-MTJ neuron is based on the magnetic field tunability of DW velocity. Simulations performed on a pair of DW-MTJ neurons show that the lateral inhibition is maximized for optimal magnetostatic interactions. To overcome the Walker breakdown (WB) limit which is the major bottleneck of the lateral inhibition efficiency, we introduce the Dzyaloshinskii-Moriya interaction (DMI) to the DW-MTJ neuron device and achieve an enhanced field tunability of the DW velocity and lateral inhibition. Such inhibition strength is sufficiently large to reverse DW motion and prevent it from firing altogether. We propose that the large inhibition parameter range is promising for yielding rich neuron firing characteristics in a DW-MTJ neuron array.

ACKNOWLEDGMENTS

The authors acknowledge funding from the National Science Foundation CAREER under Award Number 1940788, discussions and funding from Sandia National Laboratories, and computing resources from the Texas Advanced Computing Center (TACC) at The University of Texas at Austin (www.tacc.utexas.edu). Authors N Hassan and J S Friedman acknowledge National Science Foundation Award Number 1910800.

This paper describes objective technical results and analysis. Any subjective views or opinions that might be expressed in the paper do not necessarily represent the views of the U.S. Department of Energy or the United States Government. Sandia National Laboratories is a multimission laboratory managed and operated by NTESS, LLC, a wholly owned subsidiary of Honeywell International Inc., for the U.S. Department of Energy's National Nuclear Security Administration under contract DE-NA0003525.

REFERENCES

- [1] Backus, J., "Can programming be liberated from the von neumann style? A functional style and its algebra of programs," *Commun. ACM* **21**, 613–641 (1978).

- [2] Merolla, P. A., Arthur, J. V., Alvarez-Icaza, R., Cassidy, A. S., Sawada, J., Akopyan, F., Jackson, B. L., Imam, N., Guo, C., Nakamura, Y., and Brezzo, B., “A million spiking-neuron integrated circuit with a scalable communication network and interface,” *Science* **345**, 668–673 (2014).
- [3] Blouw, P., Choo, X., Hunsberger, E., and Eliasmith, C., “Benchmarking keyword spotting efficiency on neuromorphic hardware,” *Neuro-inspired Computational Elements Workshop (NICE '19)* (2019).
- [4] Mostafa, H., Müller, L. K., and Indiveri, G., “Rhythmic inhibition allows neural networks to search for maximally consistent states,” *Neural computation* **27**, 2510–2547 (2015).
- [5] Maass, W., “On the computational power of winner-take-all,” *Neural computation* **12**, 2519–2535 (2000).
- [6] de Almeida, L., Idiart, M., and Lisman, J. E., “A second function of gamma frequency oscillations: An E%-max winner-take-all mechanism selects which cells fire,” *The Journal of Neuroscience* **29**, 7497–7503 (2009).
- [7] Baars, B. J. and Gage, N. M., [*Cognition, Brain, and Consciousness*], Academic Press, Cambridge (2010).
- [8] Coultrip, R., Granger, R., and Lynch, G., “A cortical model of winnertake-all competition via lateral inhibition,” *Neural Networks* **5**, 47–54 (1992).
- [9] Mead, C. A. and Mahowald, M. A., “A silicon model of early visual processing,” *Neural Network* **1**, 91–97 (1989).
- [10] Choi, J. and Sheu, B. J., “A high-precision VLSI winner-take-all circuit for self-organizing neural networks,” *IEEE J. Solid-State Circuits* **28**, 576–584 (1993).
- [11] Ebong, I. E. and Mazumder, P., “CMOS and memristor-based neural network design for position detection,” *Proceedings of the IEEE* **100**, 2050–2060 (2011).
- [12] Currivan-Incorvia, J. A., Siddiqui, S., Dutta, S., Evarts, E. R., Zhang, J., Bono, D., Ross, C. A., and Baldo, M. A., “Logic circuit prototypes for three-terminal magnetic tunnel junctions with mobile domain walls,” *Nat. Commun.* **7**, 10275 (2016).
- [13] Sharad, M., Augustine, C., Panagopoulos, G., and Roy, K., “Spin-based neuron model with domain-wall magnets as synapse,” *IEEE Trans. Nanotechnol.* **11**, 843–853 (2012).
- [14] Sengupta, A., Shim, Y., and Roy, K., “Proposal for an all-spin artificial neural network: Emulating neural and synaptic functionalities through domain wall motion in ferromagnets,” *IEEE Trans. Biomed. Circuits Syst.* **10**, 1152–1160 (2016).
- [15] Hassan, N., Hu, X., Jiang-Wei, L., Brigner, W. H., Akinola, O. G., Garcia-Sanchez, F., Pasquale, M., Bennett, C. H., Incorvia, J. A. C., and Friedman, J. S., “Magnetic domain wall neuron with lateral inhibition,” *Journal of Applied Physics* **124**, 152127 (2018).
- [16] Brigner, W. H., Hassan, N., L. Jiang-Wei, X. H., Saha, D., Bennett, C. H., Marinella, M. J., Incorvia, J. A. C., Garcia-Sanchez, F., and Friedman, J. S., “Shape-based magnetic domain wall drift for an artificial spintronic leaky integrate-and-fire neuron,” *IEEE Trans. Electron Devices* **66**, 4970–4975 (2019).
- [17] Cui, C., Akinola, O. G., Hassan, N., Bennett, C. H., Marinella, M. J., Friedman, J. S., and Incorvia, J. A. C., “Maximized lateral inhibition in paired magnetic domain wall racetracks for neuromorphic computing,” *Nanotechnology* **31**, 294001 (2020).
- [18] Engel-Herbert, R. and Hesjedal, T., “Calculation of the magnetic stray field of a uniaxial magnetic domain,” *J. Appl. Phys.* **97**, 074504 (2005).
- [19] Schryer, N. L. and Walker, L. R., “The motion of 180° domain walls in uniform dc magnetic fields,” *J. Appl. Phys.* **45**, 5406–5421 (1974).
- [20] Emori, S., Bauer, U., Ahn, S., Martinez, E., and Beach, G. S. D., “Current-driven dynamics of chiral ferromagnetic domain walls,” *Nature Materials* **12**, 611–616 (2013).
- [21] Vansteenkiste, A., Leliaert, J., Dvornik, M., Helsen, M., Garcia-Sanchez, F., and Waeyenberge, B. V., “The design and verification of MuMax3,” *AIP Adv.* **4**, 107133 (2014).